Physical properties of hexagonal WN_2 under pressure*

Li Xiao-Feng(李晓凤)[a)b)†], Zhai Hong-Cun(翟红村)[c)], Fu Hong-Zhi(付宏志)[a)], Liu Zhong-Li(刘中利)[a)], and Ji Guang-Fu(姬广富)[b)]

[a)] *College of Physics and Electronic Information, Luoyang Normal College, Luoyang* 471022, *China*
[b)] *Laboratory for Shock Wave and Detonation Physics Research, Institute of Fluid Physics, China Academy of Engineering Physics, Mianyang* 621900, *China*
[c)] *Mathematics College, Luoyang Normal College, Luoyang* 471022, *China*

(Received 13 April 2011; revised manuscript received 12 May 2011)

A first-principles study on the mechanical stability, elastic and thermodynamic properties of WN_2 with $P63/mmc$ and P-$6m2$ phases are reported using the pseudo potential plane wave method within the generalized gradient approximation. The calculated equilibrium parameters are in good agreement with the available theoretical data. A complete elastic tensor and crystal anisotropies of the ultra-incompressible WN_2 are determined in the wide pressure range. By the elastic stability criteria, it is predicted that $P6_3/mmc$ and P-$6m2$ phases in WN_2 are not stable above 175.1 GPa and 170.1 GPa, respectively. Finally, by using the quasiharmonic Debye model, the isothermal and adiabatic bulk modulus, and the heat capacity of WN_2 are also successfully obtained.

Keywords: density functional theory, elasticity, thermodynamic properties, nitrides

PACS: 31.15.A–, 62.20.de, 67.25.de, 81.05.Je **DOI:** 10.1088/1674-1056/20/9/093101

1. Introduction

Transition metal dinitrides have attracted considerable attention from both theoretical and experimental studies due to their extreme hardness and durability as well as outstanding mechanical, optical and electronic properties.[1−4] They are widely used in many applications, such as abrasives, cutting tools and scratch resistant coatings. Recently, by inserting N atoms into the interstitial sites of transition metals with a high valence-electron density (VED), platinum-metal (such as Pt, Ir, Os and Pd) dinitrides[5−8] were successfully synthesized under high pressure and temperature (in the range of 60 GPa and 2000 K). Their ultrahigh bulk moduli and anomalously low compressibility observed in experiment (428 GPa for IrN_2[7]) make them potential candidates as superhard materials. Meanwhile, a few theoretical studies[9−14] have focused on finding all of their possible structures, which are very important in the search for new superhard materials.

Until now, however, WN_2 is still not synthesized in crystalline form. For a long time it was been speculated that it would adopt a fluorite-type structure.[15] Kroll *et al.*[16] proposed two structures of baddeleyite and cotunnite types, which are superior to the fluorite-type structure. The calculated phase diagram showed that WN_2 should be synthesized above 2000 K and 30 GPa. The elastic constants and electronic structures of the monoclinic structure of WN_2 have been investigated by *ab initio* calculations.[17] The physical properties of tetragonal ReN_2 and WN_2 have been studied from first-principles calculations. It was found that the tetragonal phase should be more stable than hexagonal ones above 175 GPa.[18] Two hexagonal $P6_3/mmc$ and P-$6m2$ structures[19,20] of WN_2 with N–W–N sandwiches layers, which are more stable than the cotunnite and baddeleyite ones, are predicted by the first-principles calculations. The elastic properties of two hexagonal structures are also explored.[20] However, to our knowledge, few studies have reported on the elastic and thermodynamic properties of hexagonal structures of WN_2 under pressure. In particular, the elastic constants under pressure are very important to determine the response of the crystal to ex-

*Project supported by the National Natural Science Foundation of China (Grant No. 11047151), the Henan Research Program of Basic and Frontier Technology, China (Grant Nos. 102300410213 and 112300410024), the Natural Science Basic Research Fund of Henan Province, China (Grant No. 2011B140013), the Scientific Research Foundation of Luoyang Normal University, China (Grant No. 2010-QNJJ-003), and the Open Research Fund of State Key Laboratory of Breeding Base of Green Chemistry-Synthesis Technology, China (Grant No. GCTKF 2010017).

†Corresponding author. E-mail: lxfdjy@126.com

© 2011 Chinese Physical Society and IOP Publishing Ltd

ternal forces, as characterized by the bulk and shear modulus, and they obviously play an important role in determining the strength and hardness of materials. Moreover, it is essential for many practical applications, such as load deflection, thermoelastic stress and fracture toughness.[21] The physical properties under high pressures and temperatures have important guidable significance in accelerating the synthesis of WN_2.

Therefore, in this work, we focus on structural, elastic and thermodynamic properties of WN_2 with $P6_3/mmc$ and P-$6m2$ structures under pressures of up to 200 GPa by first-principles calculations. The elastic properties of two hexagonal structures of WN_2 under pressure are investigated for the first time, from which the mechanical stability are also determined. In order to further investigate WN_2, the thermodynamic properties, such as the heat capacity, thermal expansion, Debye temperature and Grüneisen parameters, are obtained by the Debye model. The rest of this paper is structured as follows. In Section 2, we give a brief description of the theoretical method. The results and some discussions of the structural, elastic and thermodynamic properties of WN_2 under pressure are presented in Section 3. Conclusions derived from our calculations are drawn in the last section.

2. Theoretical methods

2.1. Total energy electronic structure calculations

In our calculations, we adopt the non-local ultrasoft pseudopotential (USPP) introduced by Vanderbilt[22] for the interactions of the electrons with the ion cores, together with the Perdew–Burke–Ernzerhof (PBE) generalized gradient approximation (GGA) exchange-correlation functional.[23] The electronic wave functions are expanded in the plane-wave basis set with a cutoff energy of 800.0 eV. Pseudo atomic calculations are performed for N $2s^2 2p^3$ and W $5s^2 5p^6 5d^4 6s^2$. As for the Brillouin-zone sampling, we use the Monkhorst–Pack mesh with 12×12×12 k-points, where the self-consistent convergence of the total energy is set to be 10^{-7} eV per atom. These parameters are sufficient in leading to a well-converged total energy. All the electronic structure calculations are implemented with the CASTEP code.[24,25]

2.2. Elastic properties and Debye temperature

Elastic constants are defined by means of a Taylor expansion of the total energy, $E_{\rm t}(V, \delta)$, for the system with respect to a small strain δ of the lattice primitive cell volume V. The energy of a strained system is expressed as follows:[26]

$$E_{\rm t}(V,\delta) = E_{\rm t}(V_0,0) + V_0\left[\sum_i \tau_i\xi_i\delta_i + \frac{1}{2}\sum_{ij} C_{ij}\delta_i\xi_i\delta_j\right], \quad (1)$$

where $E_{\rm t}(V_0, 0)$ is the energy of the unstrained system with equilibrium volume V_0, τ_i is an element in the stress tensor and ξ_i is a factor to take care of the Voigt index. It is known that there are five independent components of the elastic tensor for hexagonal structure WN_2, i.e., C_{11}, C_{12}, C_{13}, C_{33} and C_{44}.

The mechanical anisotropy of WN_2 can be obtained using the bulk moduli along the a and c axes, B_a and B_c respectively, defined as

$$B_a = a\frac{{\rm d}p}{{\rm d}a} = \frac{\Lambda}{2+\alpha}, \quad (2)$$

$$B_c = c\frac{{\rm d}p}{{\rm d}c} = \frac{B_a}{\alpha}, \quad (3)$$

$$\Lambda = 2(C_{11}+C_{12}) + 4C_{13}\alpha + C_{33}\alpha^2, \quad (4)$$

$$\alpha = \frac{C_{11}+C_{12}-2C_{13}}{C_{33}-C_{13}}. \quad (5)$$

The Debye temperature may be estimated from the average sound velocity $v_{\rm m}$[27]

$$\Theta = \frac{h}{k}\left[\frac{3n}{4\pi}\left(\frac{N_{\rm A}\rho}{M}\right)\right]^{1/3} v_{\rm m}, \quad (6)$$

where h is Planck's constants, k is Boltzman's constant, $N_{\rm A}$ is Avogadro's number, n is the number of atoms per formula unit, M is the molecular mass per formula unit, ρ is the density and $v_{\rm m}$ is obtained from[27]

$$v_{\rm m} = \left[\frac{1}{3}\left(\frac{2}{v_{\rm s}^3} + \frac{1}{v_{\rm l}^3}\right)\right]^{-1/3}, \quad (7)$$

where $v_{\rm s}$ and $v_{\rm l}$ are the shear and longitudinal sound velocities, respectively.

For the hexagonal structure of WN_2, the isotropic bulk $B_{\rm V}$ and shear moduli $G_{\rm V}$ are expressed as

$$B_{\rm V} = \frac{1}{9}\left[2\left(C_{11}+C_{12}\right)+C_{33}+C_{13}\right], \quad (8)$$

$$G_{\rm V} = \frac{1}{30}(C_{11}+C_{12}+2C_{33}-4C_{13} + 12C_{44}+12C_{66}). \quad (9)$$

The isotropic bulk $B_{\rm R}$ and shear moduli $G_{\rm R}$ are expressed as

$$B_{\rm R} = \frac{(C_{11}+C_{12})\,C_{33}-2C_{13}^2}{C_{11}+C_{12}+2C_{33}-4C_{13}}, \tag{10}$$

$$\begin{aligned} G_{\rm R} &= \frac{5}{2}\big((C_{11}+C_{12})\,C_{33}-2C_{13}^2\big)^2\,C_{44}C_{66}\Big/\Big[3B_{\rm V}C_{44}C_{66} \\ &\quad +((C_{11}+C_{12})\,C_{33}-2C_{13}^2)^2(C_{44}+C_{66})\Big], \end{aligned} \tag{11}$$

respectively, where

$$C_{66} = \frac{1}{2}\,(C_{11}-C_{12})\,. \tag{12}$$

The arithmetic average of the Voigt and Reuss bounds is called the Voigt–Reuss–Hill (VRH) average and is commonly used to estimate elastic moduli of polycrystals. The VRH averages for shear modulus (G) and bulk modulus (B) are

$$G = \frac{1}{2}\,(G_{\rm R}+G_{\rm V})\,, \quad B = \frac{1}{2}\,(B_{\rm R}+B_{\rm V})\,. \tag{13}$$

The polycrystalline moduli are the arithmetic mean values of the Voigt and Reuss moduli:[28]

$$G_{\rm H} = \frac{1}{2}(G_{\rm R}+G_{\rm V}), \quad B_{\rm H} = \frac{1}{2}(B_{\rm R}+B_{\rm V}). \tag{14}$$

Therefore, the probable values of the average shear and longitudinal sound velocities can be calculated from Navier's equation[29]

$$v_{\rm s} = \sqrt{\frac{G_{\rm H}}{\rho}}, \quad v_{\rm l} = \sqrt{\frac{(B_{\rm H}+4G_{\rm H}/3)}{\rho}}. \tag{15}$$

The polycrystalline Poisson's ratio (ν), Young's modulus (E) and Lamè constants (λ) are often used for polycrystalline materials when investigating their hardness. These quantities are calculated from the following formula:

$$\begin{aligned} E &= \frac{9BG}{3B+G}, \quad \nu = \frac{3B-E}{6B}, \\ \lambda &= \frac{\nu E}{(1+\nu)(1-2\nu)}. \end{aligned} \tag{16}$$

2.3. Thermodynamic properties

To investigate the thermodynamic properties of WN_2, we apply the quasi-harmonic Debye model,[30] in which the phononic effect is considered, and the non-equilibrium Gibbs function $G^*(V;P,T)$ takes the form of

$$G^*(V;P,T) = E_{\rm t}(V) + PV + A_{\rm Vib}(\Theta(V);T), \tag{17}$$

where $E_{\rm t}(V)$ is the total energy per unit cell, PV corresponds to the constant hydrostatic pressure condition, $\Theta(V)$ is the Debye temperature and $A_{\rm Vib}$ is the vibrational Helmholtz free energy that can be written as

$$\begin{aligned} &A_{\rm Vib}(\Theta;T) \\ &= nkT\left[\frac{9}{8}\frac{\Theta}{T} + 3\ln(1-{\rm e}^{-\Theta/T}) - D(\Theta/T)\right], \end{aligned} \tag{18}$$

where $D(\Theta/T)$ is the Debye integral, n is the number of atoms per formula unit and Θ is the Debye temperature defined by Eq. (6).

By solving the following equation with respect to V, we have

$$\left(\frac{\partial G^*(V;P,T)}{\partial V}\right)_{P,T} = 0, \tag{19}$$

one could obtain the thermal equation of state, V (P, T) and the thermal expansion coefficient α as follows:

$$\alpha = \gamma C_V/(B_{\rm T}V), \tag{20}$$

where the isothermal bulk modulus $B_{\rm T}$, the heat capacity C_V and the Grüneisen parameter γ are expressed as

$$B_{\rm T}(P,T) = V\left[\frac{\partial^2 G^*(V;P,T)}{\partial^2 V^2}\right]_{P,T}, \tag{21}$$

$$C_V = 3nk\left[4D(\Theta/T) - \frac{3\Theta/T}{{\rm e}^{\Theta/T}-1}\right]. \tag{22}$$

The method has been applied to some materials successfully.[31–35]

3. Results and discussion

We performed the total energy electronic structure calculations in the range of primitive cell volume V from 0.74 V_0 to 1.20 V_0. No constraints are imposed on the c/a ratio, i.e., the lattice constants a and c are optimized simultaneously. For each volume, the corresponding equilibrium ratio c/a of WN_2 was determined by performing total energy calculations on a series of different c/a. Through these calculations, we can obtain the equilibrium parameters a, c, and the corresponding equilibrium ratio c/a of WN_2 under arbitrary pressures. The calculated lattice parameters are shown in Table 1, together with other theoretical results.[20] By fitting the calculated energy-volume data to the third-order Birch–Murnagham equation of state,[36] we obtained the bulk modulus B_0 and its pressure derivative B_0' (listed in Table 1). It is clear that our results are in good agreement with the

other theoretical results.[20] Generally, high hardness materials have a large bulk modulus. The calculated bulk modulus of $P6_3/mmc$ and P-$6m2$ phases of WN_2 (366 GPa and 371 GPa, respectively) are higher than those of synthesized ultra-incompressible materials such as ReB_2 of 354 GPa,[37] OsN_2 of 359 GPa,[38] IrN_2 of 327 GPa[39] and PtN_2 of 272 GPa.[40]

Table 1. Calculated equilibrium parameter a, c, ratio c/a, bulk modulus B_0 and pressure derivative bulk modulus B_0' of two hexagonal WN_2 compared with theoretical results at 0 GPa and 0 K.

	a/Å	c/Å	c/a	B/GPa	B_0'
	2.9384[a]	7.7993[a]	2.6545[a]	366.2[a]	4.52[a]
$P6_3/mmc$	2.934[b]	7.790[b]	2.6550[b]	364[d]	
	2.887[c]	7.711[c]	2.6709[c]	411[d]	
	2.9233[a]	3.9151[a]	1.3993[a]	371.1[a]	4.42[a]
P-$6m2$	2.928[b]	3.916[c]	1.3374	364[d]	
	2.881[c]	3.875[c]	1.3450	411[d]	

[a] Present work,[b] theoretical data from GGA,[20] [c] theoretical data from LDA,[20] [d] the results determined from elastic constants.

These results suggest the ultra-incompressible characteristic of hexagonal WN_2. To check our conjecture, the normalized volume V/V_0 of $P6_3/mmc$ and P-$6m2$ phases of WN_2 under different pressures and temperatures are exhibited in Fig. 1. It is easily found that at a given temperature the relative volume V/V_0 decreases with pressure and the relative volume V/V_0 at higher temperature is less than that at a lower temperature at the same pressure. Thus, the effects of

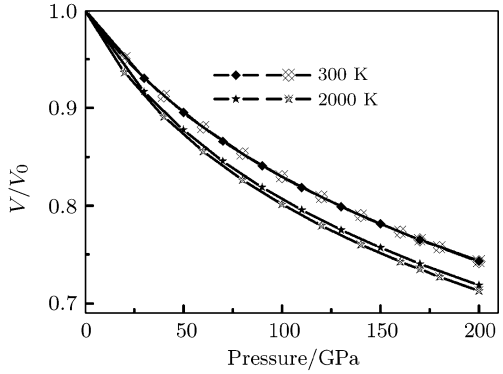


Fig. 1. The relative volume V/V_0 versus pressure for WN_2, in which solid and hollow points denote $P6_3/mmc$ and P-$6m2$ phases, respectively.

decreasing temperature of WN_2 are just the same as that of increasing pressure. For $P6_3/mmc$ and P-$6m2$ phases of WN_2, it is also seen from Fig. 1 that the relative volume V/V_0 of two structures of WN_2 are almost linear with pressure and have a nearly identical incompression in the range of pressure (0–200 GPa) at 300 K, which indicates the incompressibility of WN_2. At higher temperature (2000 K) the $P6_3/mmc$ phase is more incompressible than the P-$6m2$ phases. The results indicate that this material has very low compressibility, which makes it a potential superhard material.

The five independent elastic constants of WN_2 using a stress-strain relation are obtained from the method described above. In Table 2 we list the elastic constants of the hexagonal phases of WN_2 at 0 K and 0 GPa. It is shown that our results are in good agreement with the data (GGA) reported in Ref. [20]. However, the differences between our results and that of Ref. [20] (LDA) are rather large. From Table 2, we can also see that the calculated C_{33} of hexagoanl WN_2 is larger than c-BN of 818 GPa,[41] approaching diamond of 1106 GPa.[41] The large C_{33}, which measures the c-direction resistance to linear compression, can be mainly attributed to the N2 dimers along the c-direction.

Table 2. Elastic constants C_{ij} (GPa) at 0 GPa and 0 K.

		C_{11}	C_{33}	C_{44}	C_{12}	C_{13}
	Present work	559.5	953.5	228.0	177.2	190.0
$P6_3/mmc$	Ref. [20](GGA)	579	973	233	195	211
	Ref. [20](LDA)	642	1078	262	217	252
	Present work	578.8	972.9	225.5	181.6	192.0
P-$6m2$	Ref. [20](GGA)	588	973	232	191	206
	Ref. [20](LDA)	654	1082	260	213	248

The elastic constants of two hexagonal structures in WN_2 under pressure up to 200 GPa at 0 K are presented in Fig. 2. We can see that the five independent elastic constants of two hexagonal structures in WN_2 increase monotonously with pressure except for C_{44}. C_{11} and C_{33} vary rapidly with increasing pressure, and C_{12} becomes moderate as well as C_{13}. However, C_{44} firstly increases with pressure up to about 50 GPa and then decreases under higher pressure. We also see that $C_{33} > C_{11}$ under pressure, which suggests that it is more difficult to compress along the {001} plane than along the {100} plane. The calculated values of B_a and B_c under pressure are given in Fig. 3. It can be seen that the curves of B_a and B_c versus pressure in two structures appear nearly coincident, and B_a and B_c increase monotonously with pressure.

The materials are often used in polycrystalline aggregates; therefore, it is useful to estimate the corresponding parameters of the polycrystalline species. Moreover, the polycrystalline shear modulus G, Young's modulus E and other elastic tensors have been considered to be very important parameters governing the indentation hardness. In particular,

Young's modulus is defined as the ratio between stress and strain, which is closely relevant to the stiffness of the solid, i.e., the larger the value of E, the stiffer the material. For these purposes the bulk modulus B, shear modulus G, Young's modulus E and Lamè constants λ of WN_2 under pressure, are also exhibited in Fig. 3. At 0 K and 0 GPa, the obtained high shear modulus of two hexagonal structures indicate high hardness comparable to C–BN. The Young's modulus at 0 K and 0 GPa of WN_2 in $P6_3/mmc$(P-$6m2$) phase is 566 GPa (563 GPa), which suggests that WN_2 is a stiff material. From Fig. 3 it can be also easily observed that the shear modulus G and Young's modulus E increase incipiently and decrease gently with pressure, which is due to the variation of C_{44} with pressure. In addition, the Lamè constants λ increase as the pressure increases.

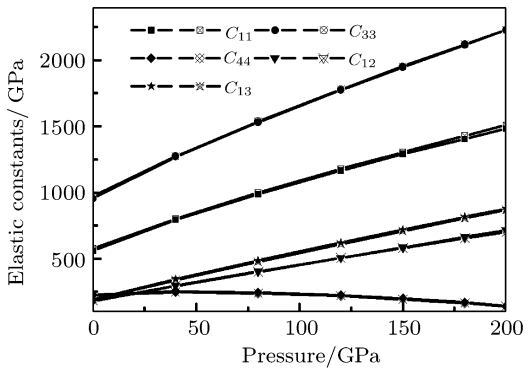


Fig. 2. Elastic constants under pressure of WN_2, in which solid and hollow points denote the $P6_3/mmc$ and P-$6m2$ phases, respectively.

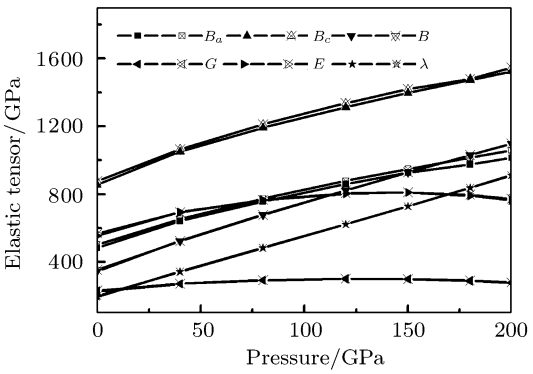


Fig. 3. The relevant elastic tensors of polycrystalline for WN_2, in which solid and hollow points denote the $P6_3/mmc$ and P-$6m2$ phases, respectively.

Poisson's ratio ν is an important parameter to describe the property of a material, the relation of Poisson's ratio ν and pressure is displayed in Fig. 4(a), from which it can be seen that Poisson's ratio ν increases monotonously under pressure. Debye temperature correlates with many physical properties of materials, such as specific heat, elastic constants and melting temperature. The Debye temperatures are derived from elastic constants under pressures (Fig. 4(b)). At zero pressure and temperature the Debye temperature of a $P6_3/mmc$ structure in WN_2 is higher with OsN_2 of 696 K,[38] IrN_2 of 649 K[39] and PtN_2 of 585 K.[40] Unfortunately, no experimental and theoretical data of elastic tensor under pressure are available for our comparison.

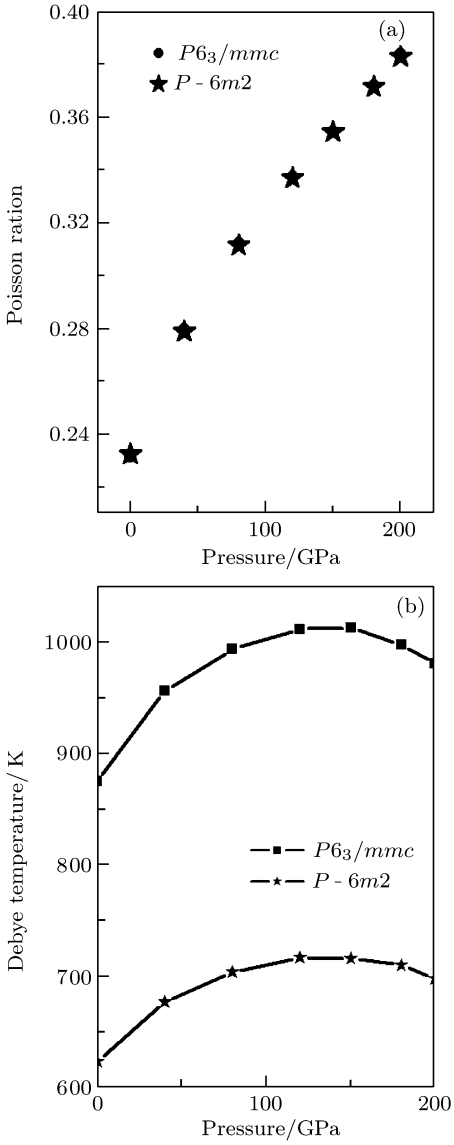


Fig. 4. (a) Poisson ratio and (b) Debye temperture under different pressures.

The ratio between the bulk and the shear modulus B/G are used to predict the brittle or ductile behaviour of materials. According to the Pugh criterion,[42] the ductile behaviour is predicted when $B/G > 1.75$, otherwise the material behaves in a brittle manner. The relations of B/G and pressure in WN_2 is exhibited in Fig. 5(a). It is obvious that the

curves of the $P6_3/mmc$ and P-$6m2$ phases nearly superpose under pressure. The ration of B/G in hexagonal structures of WN_2 increases with pressure, which is less than 1.75 under low pressure (around 24 GPa). The results indicate that hexagonal WN_2 is prone to brittleness at low pressure and is strongly prone to ductility at high pressure.

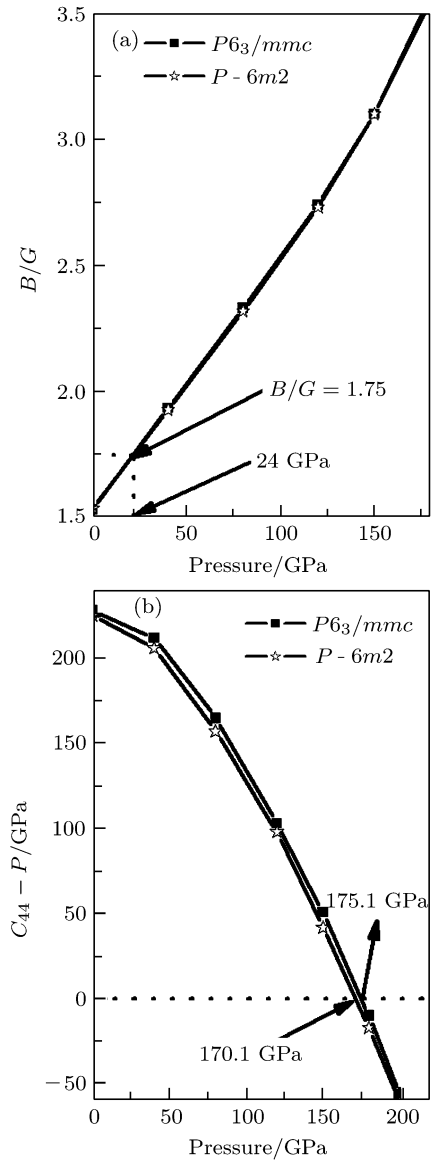


Fig. 5. (a) B/G and (b) $C_{44} - P$ versus pressures.

As is known, for hexagonal crystals, the mechanical stability under isotropic pressure can be judged from the following criterion:[43]

$$\tilde{C}_{44} > 0,\ \tilde{C}_{11} > \left|\tilde{C}_{12}\right|,\ \tilde{C}_{33}(\tilde{C}_{11}+\tilde{C}_{12}) > 2\tilde{C}_{13}, \quad (23)$$

where $\tilde{C}_{\alpha\alpha} = C_{\alpha\alpha} - P(\alpha = 1, 4)$, $\tilde{C}_{12} = C_{12} + P$, $\tilde{C}_{13} = C_{13} + P$. By fitting $\tilde{C}_{44}$ data to second-order polynomials, we have the following relations:

$$\tilde{C}_{44} = \alpha + \beta P - \gamma P^2. \quad (24)$$

Figure 5(b) shows $\tilde{C}_{44}$ versus pressures for WN_2. When the pressure $\tilde{C}_{44} > 0$ is no longer fulfilled, indicating that the $P6_3/mmc$ and P-$6m2$ phases in WN_2 are not mechanically stable at pressures of about 175.1 GPa and 170.1 GPa, respectively. The results are in good agreement with those reported in Ref. [18].

It is known that acoustic velocities are obtained from elastic constants by solving the Christoffel equation.[44] For the hexagonal phase the anisotropy of compressional wave is obtained from

$$\Delta_{\rm p} = \frac{C_{33}}{C_{11}}. \quad (25)$$

The anisotropies of the wave polarized perpendicular to the basal plane ($S1$) and the polarized basal plane ($S2$) are calculated

$$\Delta_{S1} = \frac{C_{11} + C_{33} - 2C_{13}}{4C_{44}}, \quad \Delta_{S2} = \frac{2C_{44}}{C_{11} - C_{12}}. \quad (26)$$

The dependences of the calculated three types of anisotropies of elastic waves $\Delta_{\rm p}$, Δ_{S1} and Δ_{S2} on pressure for $P6_3/mmc$ and P-$6m2$ phases are listed in Table 3. From Table 3 it can be observed that $\Delta_{\rm p}$ and Δ_{S2} decrease with increasing pressures, in which Δ_{S2} changes sharply but $\Delta_{\rm p}$ is relatively moderate. However, Δ_{S1} increases rapidly with pressure. This indicates the strong covalent bonding between N–N bonding in the nitride layer in WN_2.

Table 3. Anisotropy factors $\Delta_{\rm p}$, Δ_{S1} and Δ_{S2} for hexagonal $P6_3/mmc$ and P-$6m2$ phases of WN_2 as a function of pressure.

	$P6_3/mmc$			P-$6m2$		
	$\Delta_{\rm p}$	Δ_{S1}	Δ_{S2}	$\Delta_{\rm p}$	Δ_{S1}	Δ_{S2}
0	1.7048	1.2412	1.1937	1.68339	1.29889	1.1335
40	1.5995	1.3611	1.0141	1.5925	1.42073	0.97233
80	1.5517	1.5775	0.8419	1.54162	1.66667	0.79397
120	1.5232	1.9025	0.6778	1.51147	1.99083	0.64785
150	1.5085	2.2413	0.5694	1.49693	2.39583	0.52966
180	1.5078	2.7735	0.4613	1.48286	2.97546	0.4201

By the quasi-harmonic Debye model, the thermodynamic properties of $P6_3/mmc$ and P-$6m2$ phases in WN_2 are calculated at arbitrary pressures and temperatures. We investigated the thermodynamic quantities of $P6_3/mmc$ and P-$6m2$ phases in WN_2 under different pressures and temperatures (in the range of 0–170 GPa and 0–2000 K). Figure 6 displays the dependences of isothermal and adiabatic bulk modulus ($B_{\rm T}$, $B_{\rm S}$) on temperature at zero pressure. It is easily found that $B_{\rm T}$ and $B_{\rm S}$ are equal in amount from 0 K to 100 K and then decrease almost linearly

with increasing temperature, as is obvious from the relationship $B_{\rm S} = B_{\rm T}(1 + \alpha\gamma T)$. $B_{\rm T}$ and $B_{\rm S}$ coincide at low temperature and then diverge with rising T.

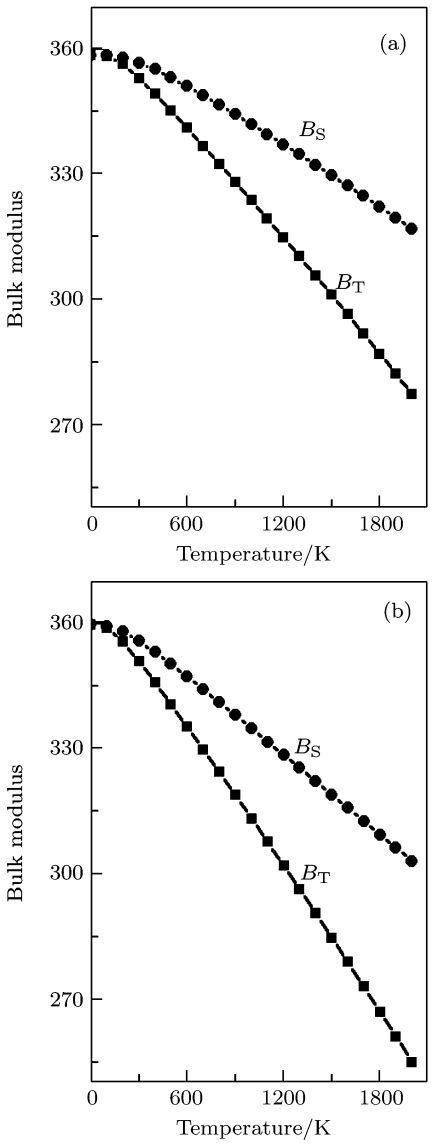


Fig. 6. Temperature dependence of isothermal ($B_{\rm T}$) and adiabatic ($B_{\rm S}$) zero-pressure bulk modulus for WN_2: (a) $P6_3/mmc$, (b) P-$6m2$.

It is found that the relationships between bulk modulus and pressure are nearly linear at various temperatures. The bulk modulus decreases with increasing temperature at a given pressure and increases with increasing pressure at a given temperature. These results are due to the fact that the effect of increasing pressure on the material is the same as that of decreasing temperature on it.

The knowledge of the heat capacity of a crystal not only provides essential information on its vibrational properties but also is mandatory for many applications. The relations of the heat capacity at constant pressure C_P and at constant volume C_V with temperature and pressure are shown in Fig. 7.

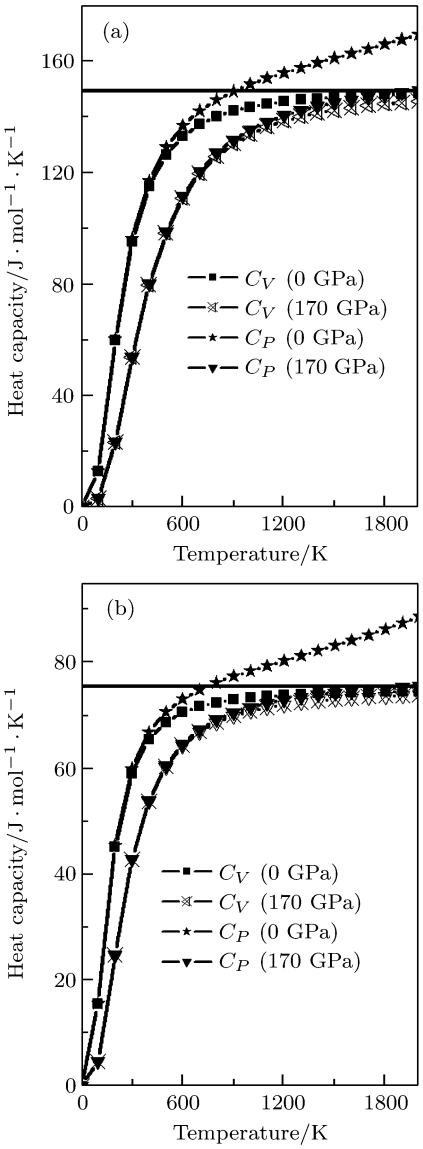


Fig. 7. Variation of heat capacity C_P and C_V under different pressures and temperatures for WN_2: (a) $P6_3/mmc$, (b) P-$6m2$.

It is seen that the difference between the constant-pressure heat capacity C_P and constant-volume heat capacity C_V is almost zero from 0 K to 600 K at the same pressure, but under higher temperatures the difference increases almost linearly with temperature. As the pressure increases, the differences between them decrease. Moreover, due to the anharmonic approximations of the Debye model at higher temperatures, the constant-volume heat capacity C_V is very close to a constant, which is the so-called Dulong–Petit limit.

4. Conclusions

In summary, the elastic and thermodynamic properties of ultra-incompressible $P6_3/mmc$ and P-$6m2$

phases in WN_2 under different pressures have been predicted by first-principles calculations for the first time. With a generalized gradient approximation for exchange and correlation, the ground state properties and equation of state of two hexagonal structures in WN_2 were obtained, which is in good agreement with theoretical calculations. The elastic constants C_{ij}, the aggregate elastic modulus B, G, E, Possion ratio ν, Debye temperature Θ and elastic anisotropies ($\Delta_{\rm p}$, Δ_{S1}, Δ_{S2}) of the hexagonal WN_2 at different pressures are also predicted. To the best of our knowledge, there is no experimental data available for these quantities. By the high pressure elastic constants, $P6_3/mmc$ and P-$6m2$ phases in WN_2 are not mechanically stable at pressures above 175.1 GPa and 170.1 GPa, respectively. The elastic anisotropies $\Delta_{\rm p}$ and Δ_{S2} decrease except for Δ_{S1} in the whole range of studied pressures. Experiments are expected to validate the present numerical data. In addition, the thermodynamic properties of $P6_3/mmc$ and P-$6m2$ phases in WN_2 are also predicted successfully. The dependences of heat capacity, and isothermal and adiabatic bulk modulus on pressure and temperature are obtained systematically in the ranges of 0–170 GPa and 0–2000 K. Our results will stimulate further experimental and theoretical work looking for new superhard materials in the future.

References

[1] Crowhurst J C, Goncharov A F, Sadigh B, Evans C L Morrall P G, Ferreira J L and Nelson A J 2006 *Science* **311** 1275

[2] Jhi S H, Ihm J, Louie S G and Cohen M L 1999 *Nature* **399** 132

[3] Eremets M I, Gavriliuk A G, Trojan I A, Dzivenko D A and Boehler R 2004 *Nature Mater.* **3** 558

[4] Kroll P 2003 *Phys. Rev. Lett.* **90** 125501

[5] Gregoryanz E, Sanloup C, Somayazulu M, Badro J, Fiquet G, Mao H K and Hemeley R 2004 *Nature Mater.* **3** 294

[6] Dubrovinsky L S, Dubrovinskaia N A, Swamy V, Muscat J, Harrison R, Ahuja B, Holm B and Johansson B 2001 *Nature* **410** 653

[7] Young A F, Sanloup C, Gregoryanz E, Scandolo S, Hemley R J and Mao H K 2006 *Phys. Rev. Lett.* **96** 155501

[8] Crowhurst J C, Goncharov A F, Sadigh B, Zaug J M, Aberg D, Meng Y and Prakapenka V B 2008 *J. Mater. Res.* **23** 1

[9] Yu R, Zhan Q and Zhang X F 2006 *Appl. Phys. Lett.* **88** 051913

[10] Young A F, Montoya J A, Sanloup C, Lazzeri M, Gregoryanz E and Scandolo S 2006 *Phys. Rev.* B **73** 153102

[11] Appen J V, Lumey M W and Dronskowski R 2006 *Angew.Chem., Int. Ed.* **45** 4365

[12] Chen Z W, Guo X J, Liu Z Y, Ma M Z, Jing Q, Li G, Zhang X Y, Li L X, Wang Q, Tian Y J and Liu R P 2007 *Phys. Rev.* B **75** 054103

[13] Wang Y X, Arai M, Sasaki T and Fan C Z 2007 *Phys. Rev.* B **75** 104110

[14] Aberg D, Sadigh B, Crowhurst J and Goncharov A F 2008 *Phys. Rev. Lett.* **100** 095501

[15] Meyer R J, Peters F, Gmelin L, Pietsch E and Becke-Goehring M 1933 *Gmelins Handbuch der Anorganischen Chemie* (Berlin: Springer-Verlag) p. 154

[16] Kroll P, Schröter T and Peters M 2005 *Angew. Chem. Int. Ed.* **44** 4249

[17] Lu S and Wang Y X 2010 *Phys. Status Solidi* B **247** 54

[18] Du X P, Wang Y X and Lo V C 2010 *Phys. Lett.* A **374** 2569

[19] Li Q, Wang H and Ma Y M 2010 *Journal of Superhard Materials* **32** 192

[20] Wang H, Li Q, Li Y W, Xu Y, Cui T, Oganov A R and Ma Y M 2009 *Phys. Rev.* B **79** 132109

[21] Louail L, Maouche D, Roumili A and Sahraoui F A 2004 *Mater. Lett.* **58** 2975

[22] Vanderbilt D 1990 *Phys. Rev.* B **41** 7892

[23] Perdew J P and Wang Y 1992 *Phys. Rev.* B **45** 13244

[24] Payne M C, Teter M P, Allen D C, Arias T A and Joannopoulos J D 1992 *Rev. Mod. Phys.* **64** 1045

[25] Milman V, Winkler B, White J A, Packard C J, Payne M C, Akhmatskaya E V and Nobes R H 2000 *Int. J. Quantum Chem.* **77** 895

[26] Fast L, Wills J M, Johansson B and Eriksson O 1995 *Phys. Rev.* B **51** 17431

[27] Anderson O L 1963 *J. Phys. Chem. Solids* **24** 909

[28] Hill R 1952 *Proc. Soc. London* A **65** 350

[29] Panda K B and Ravi Chandran K S 2006 *Comput. Mater. Sci.* **35** 134

[30] Blanco M A, Francisco E and Luana V 2004 *Comput. Phys. Commun.* **158** 57

[31] Chen D, Chen J D, Zhao L H, Wang C L, Yu B H and Shi D H 2009 *Chin. Phys.* B **18** 738

[32] Yu B H and Chen D 2011 *Chin. Phys.* B **20** 030508

[33] Li X F, Peng W M, Shen X M, Ji G F and Zhao F 2009 *Acta Phys. Sin.* **58** 2660 (in Chinese)

[34] Wang H Y, Cui H B, Li C Y, Li X S and Wang K F 2009 *Acta Phys. Sin.* **58** 5598 (in Chinese)

[35] Zhang W, Cheng Y, Zhu J and Chen X R 2009 *Chin. Phys.* B **18** 1207

[36] Birch F 1947 *Phys. Rev.* **71** 809

[37] Wang Y X 2007 *Appl. Phys. Lett.* **91** 101904

[38] Wang Y X, Arai M and Sasaki T 2007 *Appl. Phys. Lett.* **90** 061922

[39] Wu Z J, Zhao E J, Xiang H P, Hao X F, Liu X J and Meng J 2007 *Phys. Rev.* B **76** 054115

[40] Yu R, Zhan Q and Zhang X F 2006 *Appl. Phys. Lett.* **88** 051913

[41] Liang Y C and Zhang B 2007 *Phys. Rev.* B **76** 132101

[42] Pugh S F 1954 *Philos. Mag.* **45** 823

[43] Sinko G V and Smirnow N A 2002 *J. Phys.: Condens. Matt.* **14** 6989

[44] Auld M A 1973 *Acoustic Fields and Waves in Solids* (New York: Wiley) Vol. I